

000 001 002 003 004 005 DISENTANGLED SKILL REPRESENTATIONS FOR PRE- 006 DICTIVE HUMAN MODELING 007 008 009

010 **Anonymous authors**
011 Paper under double-blind review
012
013
014
015
016
017
018
019
020
021
022
023
024
025
026
027

ABSTRACT

011 Understanding human skill is essential for AI systems that collaborate with, coach,
012 or assist people. Unlike typical latent variable estimation problems—which rely
013 on single observations or explicit labels—skill is a persistent, compositional, and
014 behaviorally grounded construct that must be inferred from patterns over time.
015 We introduce Skill Abstraction with Interpretable Latents (**SAIL**), a method for
016 learning disentangled skill representations from naturalistic behavioral data. Our
017 approach produces a skill embedding that is robust to spurious performance fluctu-
018 ations and captures core, transferable representation of human subskills. Further-
019 more, **SAIL** supports skill-informed behavior prediction that generalizes across a
020 variety of contexts. We represent each individual with a persistent skill embed-
021 ding that controls a blend between expert and novice behavior bases and is trained
022 using counterfactual subskill swaps for disentanglement. This design yields a
023 representation that is both robust to performance variation and structured for in-
024 terpretability. We demonstrate that **SAIL** outperforms prior methods across two
025 domains—high-performance driving and baseball batting—producing skill repre-
026 sentations that are stable, predictive, and interpretable.
027

028 1 INTRODUCTION 029

030 AI systems that support, collaborate with, or coach humans must infer skill from behavior to per-
031 sonalize instruction, coordinate effectively, and adapt assistance to user ability. Yet skill is difficult
032 to model: it is latent, temporally extended, and behaviorally grounded, requiring inference from
033 patterns across multiple trials rather than individual outcomes. Moreover, skill has a compositional
034 structure, reflecting subskills that improve at different rates or shape distinct aspects of behavior.
035 These properties distinguish human skill from other variables in representation learning (e.g., ob-
036 ject identity in computer vision or task-level skills in robotics) and make its assessment critical for
037 personalization.

038 Unlike in robotics, where “skill” often refers to reusable action primitives or options (Botteghi et al.,
039 2025; Lesort et al., 2018), we focus on *human skill*, a persistent, individual-level construct composed
040 of distinct subskills that evolve at different rates and shape different aspects of behavior (Newell,
041 1991; Ericsson et al., 1993). Unlike performance, which can vary trial to trial, skill must be inferred
042 from patterns across time, making its stable representation particularly challenging.¹

043 Our desiderata for skill modeling as a representation learning problem are as follows: (1) **Construct**
044 **Validity (Messick, 1995)**: The representation should capture human skill while remaining robust
045 to noise and style, varying across individuals but stable across sessions and contexts for the same
046 person. (2) **Predictive Utility**: The learned representations should have good predictive power and
047 support forecasting of behavior observations and outcomes. (3) **Interpretability**: The representa-
048 tions should yield disentangled subcomponents corresponding to distinct subskills that can be easily
049 identified by human experts.

050 To satisfy these desiderata, we introduce Skill Abstraction with Interpretable Latents or **SAIL**. **SAIL**
051 is explicitly designed to promote construct validity, generalization, and interpretability in the learned
052

053 ¹In psychology and motor-learning theory, performance is considered a transient expression of skill influ-
054 enced by situational factors (Iso-Ahola, 2024; Fitts & Posner, 1967) We adopt this usage throughout.

skill representation. **SAIL** learns a persistent individual-level skill embedding. This design aggregates information across multiple behavioral observations from an individual, allowing the model to abstract away trial-level noise and capture consistent, long-term behavioral tendencies that reflect true skill yielding a stable learned representation. While simple aggregation methods (e.g., averages or Elo scores) can smooth variability, they conflate skillful risk-taking with poor performance. For example, a spinout in racing may raise average lap time even though it reflects an expert pushing the vehicle to its limits. Our approach learns a structured skill representation that contextualizes such events—abstracting away trial-level noise while preserving the subskill structure necessary to explain and predict behavior.

Rather than decoding behavior directly from the learned skill embedding, **SAIL** predicts behavior as a blend of canonical novice and expert behaviors. The intuition behind the blending formalism is that it removes low-level behavioral variability and forces the representation to encode structured, high-level skill-relevant variation. Overall, the model learns not only to capture general ability via the skill embedding but also how it maps onto behavior in different contexts. To encourage interpretability and disentanglement, we supervise the skill space with behaviorally grounded subskill metrics and introduce a counterfactual training strategy. This counterfactual procedure ensures that each latent dimension governs a distinct and identifiable aspect of skill.

We evaluate **SAIL** in both a high-performance driving domain and a baseball batting domain. Sports provide a natural testbed for skill modeling: success depends on mastering multiple subskills, and expertise is expressed through consistent, structured patterns of behavior. These domains also offer rich, multimodal data that capture both outcomes and the processes that generate them, and success can be quantified in well-defined terms such as lap time, ranking, or batting performance.

In this work we contribute the following:

1. Formulate human skill modeling as a representation learning problem, with explicit desiderata of construct validity, predictive utility, and subskill interpretability.
2. Propose **SAIL**, a method that combines person-level embeddings, expert–novice basis blending, and counterfactual subskill swapping to induce a disentangled and predictive skill space.
3. Demonstrate effectiveness across two distinct domains—high-performance driving and baseball—and show that **SAIL** outperforms baselines in producing skill representations that are stable, generalizable, and interpretable.

2 RELATED WORK

Modeling human skill is a long-standing challenge across education, sports science, robotics, and human–AI interaction Anderson (2014); Ericsson et al. (1993). Skill is a latent construct that can be inferred from behavior over time Newell (1991); Schmidt et al. (2018). Traditional metrics for capturing ability such as completion time, accuracy, or error rates Fitts & Posner (1967) are noisy and context-dependent and tend to capture *performance* rather than true skill. Psychometric methods like Item Response Theory and Bayesian Knowledge Tracing Embretson & Reise (2013); Corbett & Anderson (1994); Piech et al. (2015) provide principled ability estimates but remain tied to discrete items.

More advanced approaches such as trajectory clustering and inverse reinforcement learning (IRL) Ziebart et al. (2008); Abbeel & Ng (2004) aim to uncover latent behavioral structure, and extensions using probabilistic embeddings introduce latent variables z that can be interpreted as skill. However, these methods do not yield interpretable subskill structure or the granularity required for continuous motor behavior Guadagnoli & Lee (2004); Wulf (2016). Similarly, work in robot teaching emphasizes the importance of explicitly decomposing tasks into skills and subskills (Argall et al., 2009; Cakmak & Thomaz, 2012).

Representation Learning for Human Behavior: Building on general insights from representation learning Bengio et al. (2013), researchers have sought to compress sequences of states and actions into embeddings that summarize behavior Zhang et al. (2019); van den Oord et al. (2018). Autoencoders and sequence VAEs provide compressive frameworks Kingma & Welling (2013), while contrastive and self-supervised methods (e.g., CPC, SimCLR) learn robust embeddings (van den Oord et al., 2018; Chen et al., 2020b). However, these approaches operate on per-instance data,

108 often reflecting context or style rather than stable skill (Varona-Moya et al., 2021; Wu et al., 2021;
 109 Sun et al., 2024).

110 Recent work on representation learning tailored for humans and human interaction has focused
 111 on capturing behavioral regularities relevant for collaboration, including adaptation to novel part-
 112 ners Jacques et al. (2019), optimizing shared autonomy in assistive settings Gopinath et al. (2017),
 113 predictive world models of human intent for shared control DeCastro et al. (2024), and low-
 114 dimensional manifolds for intuitive shared autonomy Jeon et al. (2020). A common theme in this
 115 literature is the need to aggregate across trajectories and to use predictive objectives that capture
 116 semantic structure more effectively than reconstruction, as argued in JEPA (LeCun, 2022). Our ap-
 117 proach builds on these insights by requiring that skill embeddings demonstrate *predictive validity*:
 118 they should anticipate future behavior and downstream performance. To encourage this property,
 119 we introduce expert–novice blending as a structured inductive bias on how skill trajectories evolve.

120 **Disentangled and Interpretable Representations:** Disentanglement seeks latent dimensions that
 121 map onto distinct, interpretable factors. Methods like Beta-VAE, InfoGAN, and FactorVAE Higgins
 122 et al. (2017); Chen et al. (2016); Kim & Mnih (2018) encourage structured representations but face
 123 trade-offs in fidelity, independence, and identifiability Locatello et al. (2019). For skill modeling,
 124 this limits alignment between latent variables and subskills (Zhang et al., 2021). Recent methods
 125 such as DUSDi (Hu et al., 2024) aim to decompose skills into interpretable components affecting
 126 distinct environment factors, but challenges remain.

127 **Modeling Skill in Robotics:** Several works in reinforcement learning and robotics have explored
 128 learning latent skill spaces for control policies. Hausman et al. (2018) and Petangoda et al. (2019)
 129 learn disentangled or transferable skill embeddings to enable policy reuse and compositional action
 130 generation across tasks, while Gupta et al. (2018) develop meta-reinforcement learning strategies
 131 that encourage structured exploration. More recently, Dave & Rueckert (2025) propose a kernel-
 132 based approach for skill disentanglement within continuous control. However, these approaches
 133 address *robotic control skill* - that is, the discovery of reusable action primitives or policies for task
 134 execution - rather than *human skill* as a persistent, compositional, and interpretable construct. Our
 135 work differs fundamentally in scope and objective: SAIL seeks to model how human skill manifests,
 136 evolves, and generalizes across contexts, focusing on cognitive and behavioral interpretability rather
 137 than motor control or policy transfer.

138 Our method unifies advances in representation learning, disentanglement, and counterfactual rea-
 139 soning. By introducing participant-specific embeddings, novice–expert basis blending, and counter-
 140 factual subskill swaps, we produce skill representations that are stable, predictive, and interpretable.

143 3 APPROACH

144 **Problem Formulation:** We aim to learn a latent representation of human *skill* from behavioral
 145 data. Let $\mathcal{D} = \{\tau_1, \dots, \tau_N\}$ be a set of trajectories, where each $\tau_i = \{(s_i^t, a_i^t)\}_{t=1}^{T_i}$ is a sequence
 146 of states and actions with T timesteps and D trajectory features performed in a task context $c \in \mathcal{C}$
 147 (e.g., a racetrack or batting condition). Trajectories may include multimodal features such as vehicle
 148 telemetry, gaze, or body kinematics.

149 Our goal is to infer $z_s \in \mathbb{R}^d$ that captures stable, individual-level skill across trajectories and con-
 150 texts. We distinguish *skill*, a persistent construct, from *performance* (Iso-Ahola, 2024), which re-
 151 flects trial outcomes (e.g., lap time) and is sensitive to environmental variability. Skill should be
 152 invariant to context c while remaining *compositional*, with z_s decomposing into interpretable sub-
 153 components $z_s^{(k)}$ corresponding to distinct subskills (e.g., vehicle handling, gaze) Newell (1991);
 154 Anderson (1982). This structure enables targeted probing of specific deficiencies.

155 To connect latent subskills with behavior, we use *skill metrics* $m \in \mathcal{M}$: measurable quantities de-
 156 rived from trajectories, expert annotations, or auxiliary tasks that act as noisy proxies. For example,
 157 peak lateral g-force in a skidpad drill serves as a proxy for vehicle handling Schrum et al. (2025).
 158 Multiple metrics may map to the same subskill, providing supervision for learning structured repre-
 159 sentations of z_s . Our approach is detailed in Alg. 1

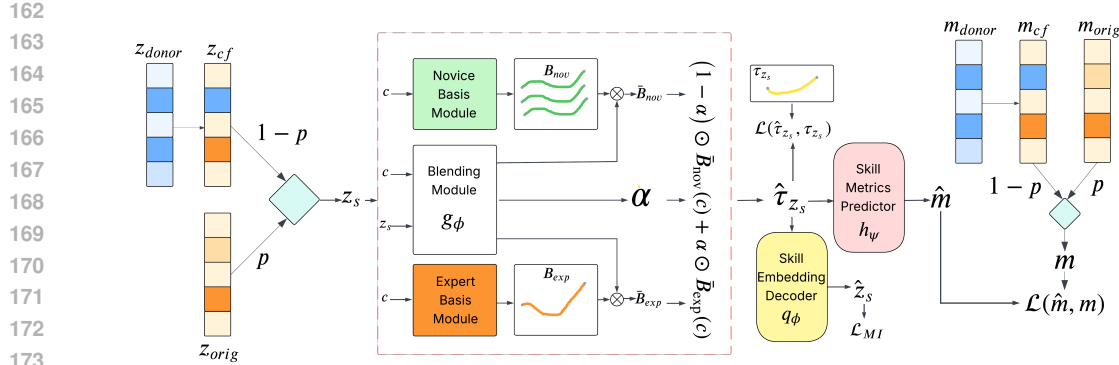


Figure 1: **SAIL** overview: Each participant is associated with a persistent skill embedding z_s that aggregates behavior across trials. This embedding controls a blend between expert and novice basis behaviors to predict trajectories, abstracting away trial-specific noise. The embedding is partitioned into subskill slices, which are supervised with behaviorally grounded skill metrics and trained using counterfactual swaps to encourage disentanglement and interpretability.

3.1 PARTICIPANT-SPECIFIC SKILL EMBEDDING

A naïve approach to skill representation would be to encode each behavioral trajectory into a latent space. However, single trajectories often reflect transient influences such as noise, fatigue, or environmental variation, making representation learning from single trajectories more suitable for capturing performance as opposed to stable skill characteristics. Moreover, isolated trajectories contain no inherent link to the individual who produced them, which is essential if skill is to be modeled as a persistent, person-specific construct. To address these issues, **SAIL** assigns each participant a persistent skill vector $z_s \in \mathbb{R}^d$, learned jointly with the model parameters (Alg. 1 Line 1). This design pools information across multiple trajectories from a participant, akin to how user and speaker embeddings are learned for recommendation (Koren et al., 2009) and speech recognition systems (Snyder et al., 2018), abstracting away trial-level variability and capturing the long-term participant-specific behavioral tendencies that define skill.

z_s is treated as a subject-specific learnable parameter that is refined throughout training based on behavioral evidence. At test time, the model is frozen and the behavioral trajectories loss is used to embed the test subjects. Conceptually, z_s is an explanatory variable: skill generates behavior, not the other way around. To prevent trivial collapse, we introduce an auxiliary network q_ϕ that reconstructs z_s from generated trajectories. This provides a variational lower bound on the mutual information between z_s and predicted behavior, encouraging the embedding to encode information that is both behaviorally meaningful and recoverable from observed trajectories (Kingma & Welling, 2013; Chen et al., 2016): $\mathcal{L}_{\text{MI}} = -\mathbb{E}_{\tau \sim p(\tau|z_s)}[\log q_\phi(z_s|\tau)]$.

3.2 NOVICE-EXPERT BASIS BLENDING

Our goal is to represent skill in a way that abstracts away trial-specific noise and stylistic variation while preserving stable, skill-relevant structure. We assume that observed behavior is generated from the skill embedding and lies on a spectrum that ranges from novice to expert performance. To operationalize this, we introduce a *novice-expert basis* that provides canonical reference behaviors against which individual skill can be expressed. This design rests on the assumption that skill varies in a continuous and interpolatable manner—i.e., that intermediate behaviors can be meaningfully represented as blends between novice and expert bases. While this continuity is an abstraction, it captures the intuition that progression in skill is gradual and structured, and allows our model to interpolate skill levels and generalize across individuals.

For each task context c (e.g., a racetrack in driving or batting condition in baseball), we define a set of expert and novice bases trajectories:

$$B_{\text{exp}}(c) = \{B_{\text{exp}}^{(1)}(c), \dots, B_{\text{exp}}^{(M)}(c)\}, \quad B_{\text{nov}}(c) = \{B_{\text{nov}}^{(1)}(c), \dots, B_{\text{nov}}^{(K)}(c)\},$$

216 **Algorithm 1** SAIL: Skill Abstraction with Interpretable Latents

217 **Require:** Trajectories τ_i , contexts c_i , subskill metrics m_i

218 1: Initialize participant embeddings $z_{s,i} \sim \mathcal{N}(0, 0.1)$

219 2: **for** each training iteration **do**

220 3: Sample batch of participants and trajectories

221 4: Predict behavior $\hat{\tau}_{z_s}$ via expert–novice blending (Sec. 3.2)

222 5: Decode predicted subskill metrics $\hat{m} = h_\psi(\hat{\tau}_{z_s})$

223 6: Compute total loss: $\mathcal{L} = \lambda_{\text{recon}}\mathcal{L}_{\text{traj}} + \lambda_{\text{metric}}\mathcal{L}_{\text{subskill}} + \lambda_{\text{MI}}\mathcal{L}_{\text{MI}}$.

224 7: **if** counterfactual step (probability $1 - p$) **then**

225 8: Swap subskill slice $z_{\text{orig}}^{(k)} \leftarrow z_{\text{donor}}^{(k)}$ and metric $m_{\text{orig}}^{(k)} \leftarrow m_{\text{donor}}^{(k)}$

226 9: Reconstruct counterfactual trajectory $\tilde{\tau}_{\text{orig}}$ from \tilde{z}_{orig}

227 10: **Skip trajectory reconstruction loss; apply metric loss only for swapped subskill k**

228 11: **end if**

229 12: Update model parameters and participant embeddings jointly via back-propagation

230 13: **end for**

231

232 where each basis trajectory $B^{(i)} \in \mathbb{R}^{T \times D}$ represents a canonical behavior pattern drawn from the
 233 extremes of the skill distribution, with T timesteps and D trajectory features. The expert set could in
 234 principle capture multiple distinct high-skill strategies, while the novice set spans the heterogeneous
 235 modes of novice performance (e.g., over-cautious, inconsistent, or poorly timed execution). In practice
 236 we find that a single expert basis is sufficient as expert demonstrations tend to cluster tightly
 237 around a consistent solution. In contrast, we retain multiple novice bases to capture the diversity of
 238 novice behavior.

239 These bases can be derived in multiple ways: directly from demonstration data, learned jointly with
 240 the embedding, or generated by an optimal controller. In practice, we find that a simple yet effective
 241 construction works well: (1) use trajectories from the most expert demonstrator to define B_{exp} , and
 242 (2) apply principal component analysis (PCA) to a collection of novice trajectories to define B_{nov} ,
 243 capturing the dominant axes of novice variability. This design allows the model to interpret z_s in
 244 terms of blending toward or away from the expert solution along meaningful novice dimensions.
 245 The skill embedding is then mapped into blending coefficients for each basis through a blending
 246 module network g_ϕ :

$$\alpha = g_\phi(z_s, c) \in [0, 1]^{M \times K \times T \times D}.$$

247 Finally, the predicted behavior is expressed as a weighted combination over the bases where the
 248 weights are learned via g_ϕ (Fig 1):

$$\begin{aligned} \bar{B}_{\text{exp}}(z_s, c) &= \sum_{m=1}^M w_{\text{exp}}^{(m)}(z_s, c) B_{\text{exp}}^{(m)}(c), \quad \sum_{m=1}^M w_{\text{exp}}^{(m)}(z_s, c) = 1, \quad w_{\text{exp}}^{(m)} \geq 0 \\ \bar{B}_{\text{nov}}(z_s, c) &= \sum_{k=1}^K w_{\text{nov}}^{(k)}(z_s, c) B_{\text{nov}}^{(k)}(c), \quad \sum_{k=1}^K w_{\text{nov}}^{(k)}(z_s, c) = 1, \quad w_{\text{nov}}^{(k)} \geq 0 \\ \hat{\tau}_{z_s} &= \alpha \odot \bar{B}_{\text{exp}}(z_s, c) + (1 - \alpha) \odot \bar{B}_{\text{nov}}(z_s, c), \end{aligned}$$

260 While our blending formulation references a continuum between novice and expert performance,
 261 it does not assume that skill lies on a single linear axis. We use multiple novice bases to capture
 262 diverse low-skill strategies (e.g., overcautious, inconsistent, or poorly timed behavior) and can em-
 263 ploy multiple expert basis to represent distinct high-skill styles. Each subskill dimension modulates
 264 its own blend between these bases, enabling multi-dimensional, non-linear skill representations that
 265 remain interpretable and easily extensible to domains with multiple expert styles.

266 This blending formulation (shown in the dashed box in Fig 1) shifts the focus from reproducing
 267 every trajectory detail to capturing high-level, skill-relevant structure. Behavior prediction serves as
 268 the primary training signal, tying the embedding to stable, behaviorally meaningful variation across
 269 contexts while abstracting away noise. Crucially, this predictive design also yields a structured gen-
 erative model of behavior: by intervening in the embedding space, we can probe how skill changes

would alter behavior, or hold skill fixed to forecast behavior in new contexts. These properties make the learned space useful for analysis, coaching, and simulation of counterfactual skill trajectories.

3.3 COUNTERFACTUAL TRAINING FOR SUBSKILL DISENTANGLEMENT

Human coaches diagnose deficits in specific subskills and tailor practice to address them (Ericsson et al., 1993; Newell, 1991; Wulf, 2016). More generally, effective assistance requires identifying which subcomponents of skill need improvement and designing targeted interventions (Anderson, 1982). This motivates our approach: to enable meaningful feedback, we model skill as a composition of subskills that can be selectively manipulated to predict changes in behavior.

Our goal is to learn a disentangled skill representation in which each subskill is captured by a dedicated slice of the latent space, such that manipulating that slice selectively modulates the corresponding behavior. Prior work on disentanglement, such as InfoGAN, β -VAE, and FactorVAE, has explored encouraging statistical independence between latent dimensions. While partially successful, these approaches face important drawbacks: they often limit the information capacity of the latent space Higgins et al. (2017), can be unstable to train (Locatello et al., 2019), and, crucially, do not naturally support counterfactual reasoning - that is, asking how a prediction should change if a single component of the latent space were modified Locatello et al. (2019). Even when disentanglement is encouraged, a second challenge arises: identifiability, or knowing which part of the latent space corresponds to which subskill. Conditional VAEs (Sohn et al., 2015) and related methods address this by supervising certain latent dimensions with labels (Kingma et al., 2014), anchoring them to known factors. However, this anchoring does not guarantee true disentanglement. Latent slices may still leak information about other factors, especially when labels are noisy or correlated, leading to entangled and ambiguous representations despite explicit supervision.

We propose a counterfactual training scheme motivated by Kim & Mnih (2018) that encourages both disentanglement and identifiability, while still optimizing for reconstruction accuracy. The embedding space is explicitly partitioned into subskill-specific slices,

$$z_s = [z_s^{(1)}, z_s^{(2)}, \dots, z_s^{(K)}],$$

where each slice $z_s^{(k)} \in \mathbb{R}^{d_k}$ is intended to represent subskill k , and $\sum_k d_k = d$.

Reconstructed trajectories $\hat{\tau}_{z_s}$ are mapped through a predictor network h_ψ to obtain subskill metrics \hat{m} (Fig. 1), which serve as behaviorally grounded supervision signals during training. Each skill metric is defined in collaboration with domain experts and reflects a measurable behavioral quantity that serves as a proxy for an underlying subskill (e.g., steering reversal rate for control coordination, peak lateral acceleration for vehicle handling, or gaze dispersion for visual attention). These metrics provide weak yet semantically meaningful supervision that anchors each subskill dimension to interpretable aspects of human behavior.

To enforce counterfactual consistency, we perform subskill swaps between a randomly chosen pair of training examples: an *original* sample (the one being modified) and a *donor* sample (from which a single subskill slice is borrowed). For a selected subskill k , we replace the k -th slice of the original embedding with that of the donor:

$$\tilde{z}_{\text{orig}}^{(k)} = z_{\text{donor}}^{(k)}, \quad \tilde{z}_{\text{orig}}^{(\ell)} = z_{\text{orig}}^{(\ell)} \quad \forall \ell \neq k,$$

and apply the same operation to the associated skill metrics to ensure supervision remains consistent:

$$\tilde{m}_{\text{orig}}^{(k)} = m_{\text{donor}}^{(k)}, \quad \tilde{m}_{\text{orig}}^{(\ell)} = m_{\text{orig}}^{(\ell)} \quad \forall \ell \neq k.$$

In practice, we interleave counterfactual and standard training: with probability p , a batch is trained using the regular reconstruction and metric objectives, and with probability $(1-p)$, a batch is trained with counterfactual swaps (Alg. 1, Lines 7–8). This procedure creates counterfactual examples where the original participant retains their overall embedding but adopts one subskill dimension from the donor, allowing the model to learn how isolated subskills influence predicted behavior and corresponding metrics.

This balance ensures that the model maintains reconstruction fidelity while also learning to enforce subskill disentanglement. Since no ground-truth trajectory exists for this counterfactual, we do not apply a reconstruction loss to $\hat{\tau}_{z_s}$ for the swapped batch items (Alg. 1 Line 10). Instead, the

324 predictor network, h_ψ , is required to output the swapped metric for subskill k , forcing the model to
 325 adjust behavior in a way that matches the intervention.
 326

327 Unlike approaches that impose structural constraints directly on the embedding space (e.g., linear
 328 independence penalties or orthogonality objectives), our method enforces disentanglement through
 329 behavior. The reconstructed trajectories must reproduce the correct subskill metrics, which forces
 330 each latent slice to encode and express its designated subskill in a behaviorally grounded way.
 331

332 3.4 MODELING DETAILS AND LOSSES

333 The overall training objective combines several complementary losses that promote reconstruction
 334 fidelity, semantic alignment, and disentanglement:
 335

$$336 \mathcal{L} = \lambda_{\text{traj}} \mathcal{L}_{\text{traj}} + \lambda_{\text{metric}} \mathcal{L}_{\text{metric}} + \lambda_{\text{MI}} \mathcal{L}_{\text{MI}}, \quad (1)$$

338 where $\mathcal{L}_{\text{traj}}$ is a trajectory reconstruction loss between predicted and observed behaviors, $\mathcal{L}_{\text{metric}}$
 339 supervises subskill-specific metrics predicted by h_ψ , and \mathcal{L}_{MI} is a mutual-information term encour-
 340 aging consistency between the embedding z_s and reconstructed behavior. During counterfactual
 341 training steps, $\mathcal{L}_{\text{traj}}$ is omitted since no ground-truth trajectory exists for the swapped embedding,
 342 and only the metric loss for the swapped subskill is applied.
 343

344 Our model integrates participant-level skill embeddings with trajectory and context encoders built
 345 from established sequence architectures. Contextual map features are processed using a Point-
 346 Net-Transformer encoder (Gao et al., 2020; Gopinath et al., 2025), which captures both local geom-
 347 etry and global layout. The trajectories are predicted via two decoders, which produces elementwise
 348 blending weights for expert–novice interpolation. The skill metrics predictor uses an LSTM to re-
 349 process generated trajectories and provide supervision. Architectural choices, training settings, and
 350 loss coefficients are detailed in Appendix A.2
 351

352 4 DOMAINS AND DATASETS

353 4.1 HIGH-PERFORMANCE RACING

354 High-performance racing is an ideal domain for studying skill because it requires the integration of
 355 multiple subskills under demanding conditions. We focus on six core subskills identified by expert
 356 coaches and prior work (Schrum et al., 2025): (i) vehicle handling, (ii) gaze control, (iii) know-how
 357 (strategic knowledge of racing lines and techniques), (iv) control inputs (coordination of steering,
 358 throttle, and braking), (v) physical ability, and (vi) perceptual ability. These determine a driver’s
 359 overall competence and provide a structured target for disentangled representation learning.
 360

361 Each behavioral trajectory τ_i consists of vehicle pose, speed, and control signals downsampled to
 362 100 points per track segment. The context c for this dataset refers to the racetrack that the behavioral
 363 trajectory was executed on. We collected a dataset of racing behavior from 95 participants spanning
 364 novices to experts, using a high-fidelity driving simulator. Data collection proceeded in two phases:
 365 70 participants each completed at least four laps on a single track modeled after a nearby raceway,
 366 and 25 participants each completed four laps across four distinct tracks at the same venue. This
 367 design provided both breadth (a large participant pool) and depth (multiple laps and multiple con-
 368 texts), resulting in 1545 laps. The simulator provided realistic vehicle dynamics under repeatable
 369 conditions, enabling controlled yet ecologically valid measurement of driver behavior.
 370

371 To connect observed behavior to underlying subskills, we leverage a set of behaviorally grounded
 372 skill metrics $m \in \mathcal{M}$, defined in collaboration with expert coaches (Schrum et al., 2025). Each
 373 metric is linked to a targeted task designed to probe a specific subskill: for example, peak lateral
 374 g-force in a skidpad drill reflects vehicle handling, steering reversal rate in a slalom drill reflects
 375 control input coordination, gaze fixation during driving sessions reflects gaze policy, occlusion task
 376 accuracy (where the visual scene was briefly hidden) reflects perceptual speed, dynamometer output
 377 reflects physical strength, and written test scores reflect strategic know-how of racing lines and
 378 techniques. These metrics (among others) provide partial, noisy evidence about latent subskills.
 379 Collectively, they supply the supervision signals necessary for learning structured representations of
 380 z_s .
 381

Table 1: Results across desiderata in two domains, Racing (R) and Baseball (B). Higher is better for \uparrow , lower is better for \downarrow . **Bold** = best, underline = second-best.

	SAIL (ours)		SAIL w/o CF		SAIL w/o basis		SimCLR		β-VAE		VAE		AE-LC	
	R	B	R	B	R	B	R	B	R	B	R	B	R	B
<i>Construct Validity</i>														
Silhouette (↑)	0.72		.77		0.67		0.40		0.74		0.75		0.67	
Test-retest similarity (↑)	.995	1.0	0.995	0.999	0.990	0.996	0.928	0.96	0.928	0.66	0.839	0.98	0.891	0.998
Composite (Construct) (↑)	1.86	1.0	2.0	0.997	1.69	0.99	0.57	0.88	1.49	0.00	0.95	0.94	1.06	0.99
<i>Predictive Utility</i>														
Behavior prediction (RMSE ↓)	2.76	0.24	2.75	0.22	5.05	0.32	4.15	0.29	4.48	0.26	4.61	0.26	4.87	0.31
OOC generalization (RMSE ↓)	6.37	0.33	6.50	0.29	12.77	0.48	10.27	0.38	12.51	0.30	12.42	0.36	14.12	0.37
Composite (Predictive) (↑)	2.0	1.59	1.98	2.0	0.17	0.00	0.89	0.83	0.46	1.55	0.41	1.23	0.08	0.68
<i>Disentanglement & Interpretability</i>														
Alignment Ratio (AR ↑)	3.25	2.17	1.24	1.58	1.11	1.43	1.73	0.94	1.12	0.59	1.05	1.04	2.40	1.79
Targeted Change Index (TCI ↑)	.93	0.13	0.89	0.14	0.73	0.15	0.45	0.16	0.63	0.19	0.78	0.19	0.73	.19
Relative Influence Ratio (RIR ↑)	2.11	.25	1.76	0.08	1.67	0.07	1.85	0.12	1.86	0.11	1.61	0.07	1.56	0.12
Composite (Disentangle) (↑)	3.0	2.0	1.37	0.85	0.81	0.87	0.83	1.0	0.95	1.22	0.78	1.29	1.20	2.04

4.2 BASEBALL HITTING

We applied **SAIL** to a supplemental dataset of baseball hitting collected from 13 players on a competitive adult team in a semi-professional league. While all participants were skilled and experienced players, they were not yet at the level of an expert benchmark and thus exhibited substantial variation in the execution of key subskills. One highly skilled participant was identified as an expert and used to define the canonical expert basis for blending, while the remaining players provided a diverse set of novice-to-intermediate trajectories. In total, 74 batting trials were recorded, spanning both pitching machine sessions and tee batting conditions. Whole-body kinematics of swing motions were captured using an optical motion capture system. In collaboration with a coach, we identified three core subskills and associated metrics of effective hitting: (i) the *kinematic chain*, or the sequential transfer of momentum across body segments; (ii) *pelvis pausing*, or the ability to momentarily stabilize the pelvis to build rotational power; and (iii) *thigh pausing*, or the controlled deceleration of the lead thigh to anchor lower-body mechanics. The contexts c for this dataset are batting from a tee and batting against live pitches from a machine. Unlike the racing dataset, which incorporates a broad set of tasks probing multiple subskills, this dataset is narrower in scope and primarily intended as a secondary domain to test the generality of our approach.

To address the limited size of the dataset and capture broader variability, we generated synthetic participants by applying trajectory augmentations (time warping, noise injection, and scaling) to recorded swings. For players with both tee and regular trials, we estimated a global offset between conditions and used it to synthesize additional regular swings. This procedure produced artificial batting trials that preserved the underlying structure of advanced but non-expert motion while introducing diversity reflective of natural variations in skill.

To our knowledge, there are no existing datasets that capture multimodal behavioral signals, targeted drills, and coach-aligned annotations for baseball that are comparable in richness to our racing dataset. We therefore treat this baseball dataset as supplemental—smaller in scale, narrower in subskill coverage, and heavily augmented with synthetic trials—but nevertheless valuable for demonstrating that **SAIL** can extend beyond driving to a distinct motor domain.

5 RESULTS

We compare our method against several baselines and ablations to evaluate the contribution of each component:

SimCLR (contrastive baseline). A self-supervised representation learning method that uses contrastive losses to encourage invariance within a person. We adapt SimCLR to trajectory data to test whether a generic contrastive objective is sufficient for extracting skill-relevant embeddings Chen et al. (2020a).

β -VAE (disentanglement baseline). An extension of the VAE with a stronger KL regularization term that encourages factorized latents. We include β -VAE as a canonical disentanglement method, testing whether generic disentanglement pressure yields interpretable subskills Higgins et al. (2017).

432 **AE (autoencoder baseline).** A standard trajectory auto-encoder (Kingma & Welling, 2013). This
 433 provides a comparison to unsupervised compression methods that capture per-trial variability but
 434 are not explicitly designed to model persistent skill or subskill structure Hinton & Salakhutdinov
 435 (2006).

436 **AE with linear constraints (structured baseline).** A recent extension of the
 437 autoencoder framework that incorporates linear constraints into the latent space to en-
 438 courage semantically meaningful and identifiable embeddings. We include this method
 439 to test whether such constraints help discover interpretable subskills in driving data
 440 and utilize the subskill metrics to create the linear constraints (Lin et al., 2020).
 441

442 **Ablation: without counterfactual training.** This
 443 variant removes the counterfactual swap objective,
 444 training only with behavioral prediction via the
 445 expert-novice bases blending. This isolates the
 446 contribution of counterfactual training to disentangle-
 447 ment and interpretability.

448 **Ablation: without expert–novice basis and with-
 449 out counterfactual training.** Instead of decoding
 450 trajectories as a blend of expert and novice bases,
 451 this variant decodes directly from the skill embed-
 452 ding. We also ablate the counterfactual training in
 453 this variant. This tests whether the basis decomposi-
 454 tion is necessary for isolating skill-relevant variation
 455 from noise and style.

456 For all baselines that operate at the trial level (Sim-
 457 CLR, AE, β -VAE, AE-LC), we extract embeddings
 458 per trajectory and then poll them across laps for each
 459 participant, yielding a participant-level embedding
 460 comparable to our method. We evaluate our approach and baselines along the three desiderata
 461 introduced in Section 3: (1) construct validity, (2) predictive utility, and (3) disentanglement and
 462 interpretability. Together, these evaluations assess whether the learned representation z_s is well-
 463 structured, useful for downstream tasks, and decomposable into meaningful subskills.

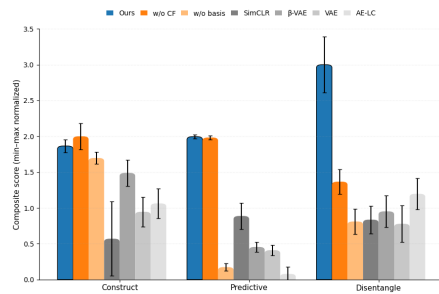
464 5.1 CONSTRUCT VALIDITY

466 We evaluate *construct validity* by measuring whether the learned embedding captures stable, skill-
 467 relevant structure rather than transient fluctuations or task-specific noise. Two complementary met-
 468 rics are reported in Table 1. Full metric definitions of the metrics are provided in Appendix A.4.

469 **In this work, we interpret construct validity in the behavioral and representational sense**—whether
 470 the learned embedding behaves consistently with the theoretical construct of human skill (i.e., stable
 471 within individuals and discriminative across skill levels)—rather than as formal psychometric val-
 472 idation. Our goal is to provide empirical evidence that the learned latent space captures skill rather
 473 than transient performance fluctuations.

- 475 • **Silhouette score** (\uparrow): clustering quality by skill group.
- 476 • **Test–retest similarity** (\uparrow): stability of embeddings across repeated trials.

478 **Discussion:** As shown in Figures 2 and Table 1, **SAIL** achieves the strongest composite score
 479 for construct validity in both racing and baseball. The participant-level embedding ensures high
 480 test–retest stability (0.995 in racing, 1.0 in baseball), reflecting that z_s captures persistent aspects
 481 of skill rather than trial-specific noise. The ablation without counterfactual training (**SAIL** w/o
 482 CF) performs comparably, which is expected since counterfactual swaps are designed to improve
 483 disentanglement rather than stability. In contrast, removing the novice–expert basis (**SAIL** w/o
 484 basis) reduces silhouette scores, likely because the embedding must capture trial-level variability
 485 instead of abstracting away noise. Baselines such as SimCLR cluster trials from the same participant
 but may emphasize stylistic consistency rather than stable skill, while autoencoder variants show



460 Figure 2: Composite scores across the three
 461 desiderata: construct validity, predictive utility,
 462 and disentanglement/interpretability. Bars show performance of our method
 463 (**SAIL**), ablations (w/o CF, w/o basis), and
 464 baselines (SimCLR, β -VAE, VAE, AE-LC).
 465 Higher is better for all desiderata.

486 some separation but less interpretability. Overall, these results confirm that anchoring skill at the
 487 participant level and incorporating basis blending is key to achieving construct validity.
 488

489 **5.2 PREDICTIVE UTILITY**
 490

491 We next assess *predictive utility* by evaluating whether the learned skill embeddings support accurate
 492 trajectory forecasting within and across contexts.

493

- 494 • **In-context prediction (RMSE \downarrow)**: trajectory accuracy within the same context.
- 495 • **Out-of-context prediction (RMSE \downarrow)**: generalization to novel contexts.

496 **Discussion:** As shown in Figures 2 and Table 1, **SAIL** achieves the lowest error for both in-context
 497 and out-of-context prediction, confirming that the learned embeddings capture stable behavioral ten-
 498 dencies that generalize across settings. The ablation without counterfactual training (**SAIL** w/o CF)
 499 performs similarly on predictive metrics, consistent with the design of counterfactual swaps, which
 500 target disentanglement rather than raw forecasting. By contrast, removing the novice-expert basis
 501 (**SAIL** w/o basis) substantially degrades prediction, with errors nearly doubling in the racing do-
 502 main. This highlights that basis blending is critical for abstracting away trial-level variability and
 503 anchoring z_s in structured behavioral dimensions. Baselines show weaker generalization: autoen-
 504 coder variants (VAE, β -VAE, AE-LC) capture per-trial variability but fail to transfer to new contexts.
 505 Together, these results demonstrate that predictive validity is best achieved by combining person-
 506 level embeddings with structured novice-expert bases. Notably, predictive utility is not significantly
 507 reduce by our counterfactual training scheme, suggesting that it may encourage disentanglement
 508 without greatly hurting prediction accuracy. AE-LC on the other hand performs the worst in terms
 509 of predictive utility.

510 **5.3 DISENTANGLEMENT AND INTERPRETABILITY**
 511

512 Finally, we evaluate whether the representation decomposes into interpretable subcomponents that
 513 correspond to distinct subskills. Three complementary metrics are reported in Table 1:

514

- 515 • **Alignment Ratio (AR \uparrow)**: measures how well each subskill slice $z_s^{(k)}$ predicts its intended
 516 metrics compared to non-target ones, indicating subskill-metric correspondence.
- 517 • **Targeted Change Index (TCI \uparrow)**: quantifies the effect of counterfactual swaps by checking
 518 whether trajectory changes are concentrated in the targeted features, with higher values
 519 reflecting more selective control.
- 520 • **Relative Influence Ratio (RIR \uparrow)**: compares the relative impact of subskills on over-
 521 lapping behavioral outputs (e.g., control inputs vs. gaze), capturing whether slices exert
 522 influence in proportion to their intended role.

523 **Discussion:** Figures 2 and Table 1 show that **SAIL** consistently achieves the highest disentangle-
 524 ment scores in racing, while differences are smaller in baseball. This gap can be explained by
 525 the nature of the datasets. The baseball data is smaller in scale and includes substantial synthetic
 526 augmentation, which produces clearer, more linearly separable relationships between metrics and
 527 behavior. As a result, structured baselines such as AE-LC are able to capture some of these rela-
 528 tionships without the need for counterfactual supervision, narrowing the gap. By contrast, the racing
 529 domain contains richer and more heterogeneous variability, making counterfactual swaps essential
 530 for learning interpretable subskill slices. Overall, these results suggest that counterfactual super-
 531 vision is particularly valuable in complex, high-variance settings, whereas in simpler or synthetic
 532 domains, weaker baselines can exploit linear structure to partially mimic disentanglement.

533 **6 LIMITATIONS**
 534

535 Our evaluation is limited by dataset scale and scope, particularly in the baseball domain where data
 536 are small and augmented. The method also depends on noisy, predefined subskill metrics, and as-
 537 sumes a smooth novice-expert continuum that may overlook abrupt shifts or alternative strategies.
 538 Finally, while counterfactual training improves interpretability, it does not guarantee fully disentan-
 539 gled subskills.

540 REPRODUCIBILITY STATEMENT
541542 We have taken several steps to ensure the reproducibility of our results. All datasets used in our
543 experiments are described in detail in Section 4 and Section A.3. Model architectures, hyperparam-
544 eters, and training configurations are reported in Section 3 and further detailed in Appendix A.2.
545546 REFERENCES
547548 Pieter Abbeel and Andrew Y Ng. Apprenticeship learning via inverse reinforcement learning. In
549 *ICML*, pp. 1–8, 2004.551 John R. Anderson. Acquisition of cognitive skill. *Psychological Review*, 89(4):369–406, 1982.552 John R Anderson. *Learning and memory: An integrated approach*. John Wiley & Sons, 2014.554 Brenna D. Argall, Sonia Chernova, Manuela Veloso, and Brett Browning. A survey of robot learning
555 from demonstration. *Foundations and Trends in Robotics*, 1(4):1–157, 2009. doi: 10.1561/
556 2300000013.558 Yoshua Bengio, Aaron Courville, and Pascal Vincent. Representation learning: A review and new
559 perspectives. *IEEE Transactions on Pattern Analysis and Machine Intelligence*, 35(8):1798–1828,
560 2013.561 Nicolò Botteghi et al. Unsupervised skill discovery: A review. *Robotics and Autonomous Systems*,
562 2025.564 Maya Cakmak and Andrea L. Thomaz. Designing robot learners that ask good questions. In *Pro-
565 ceedings of the 7th Annual ACM/IEEE International Conference on Human-Robot Interaction
566 (HRI)*, pp. 17–24, 2012. doi: 10.1145/2157689.2157693.568 Ting Chen, Simon Kornblith, Mohammad Norouzi, and Geoffrey Hinton. A simple framework for
569 contrastive learning of visual representations. In *International Conference on Machine Learning
570 (ICML)*, pp. 1597–1607, 2020a.571 Ting Chen, Simon Kornblith, Mohammad Norouzi, and Geoffrey Hinton. A simple framework for
572 contrastive learning of visual representations. In *ICML*, pp. 1597–1607, 2020b.574 Xi Chen, Yan Duan, Rein Houthooft, John Schulman, Ilya Sutskever, and Pieter Abbeel. Infogan:
575 Interpretable representation learning by information maximizing generative adversarial nets. In
576 *NeurIPS*, 2016.578 Albert T Corbett and John R Anderson. Knowledge tracing: Modeling the acquisition of procedural
579 knowledge. *User Modeling and User-Adapted Interaction*, 4:253–278, 1994.580 Vishnu Dave and Elmar Rueckert. Skill disentanglement in reproducing kernel hilbert space. In
581 *Proceedings of the AAAI Conference on Artificial Intelligence*, volume 39, pp. 16153–16162,
582 2025.584 Jonathan DeCastro, Andrew Silva, Deepak Gopinath, Emily Sumner, Thomas M. Balch, Laporsha
585 Dees, and Guy Rosman. Dreaming to assist: Learning to align with human objectives for shared
586 control in high-speed racing. In *Conference on Robot Learning (CoRL)*, 2024. URL <https://arxiv.org/abs/2410.10062>.588 Susan E Embretson and Steven P Reise. *Item response theory for psychologists*. Psychology Press,
589 2013.591 K Anders Ericsson, Ralf T Krampe, and Clemens Tesch-Römer. The role of deliberate practice in
592 the acquisition of expert performance. *Psychological Review*, 100(3):363–406, 1993.593 Paul M Fitts and Michael I Posner. *Human performance*. Brooks/Cole, 1967.

594 Jiyang Gao, Chen Sun, Hang Zhao, Yi Shen, Dragomir Anguelov, Congcong Li, and Cordelia
 595 Schmid. Vectornet: Encoding hd maps and agent dynamics from vectorized representation. In
 596 *Proceedings of the IEEE/CVF conference on computer vision and pattern recognition*, pp. 11525–
 597 11533, 2020.

598 Deepak Gopinath, Siddhartha Jain, and Brenna Argall. Human-in-the-loop optimization of shared
 599 autonomy in assistive robotics. In *Proceedings of the IEEE International Conference on Robotics
 600 and Automation (ICRA)*, pp. 3925–3932, 2017. doi: 10.1109/ICRA.2017.7989426.

602 Deepak Gopinath, Xiongyi Cui, Jonathan DeCastro, Emily Sumner, Jean Costa, Hiroshi Yasuda,
 603 Allison Morgan, Laporsha Dees, Sheryl Chau, John Leonard, et al. Computational teaching for
 604 driving via multi-task imitation learning. In *2025 IEEE International Conference on Robotics and
 605 Automation (ICRA)*, pp. 7019–7027. IEEE, 2025.

606 Mark A Guadagnoli and Timothy D Lee. Challenge point: A framework for conceptualizing the
 607 effects of various practice conditions in motor learning. *Journal of Motor Behavior*, 36(2):212–
 608 224, 2004.

609 Abhishek Gupta, Russell Mendonca, YuXuan Liu, Pieter Abbeel, and Sergey Levine. Meta-
 610 reinforcement learning of structured exploration strategies. In *Advances in Neural Information
 611 Processing Systems (NeurIPS)*, volume 31, pp. 5302–5311, 2018.

612 Karol Hausman, Yevgen Chebotar, Stefan Schaal, Gaurav S Sukhatme, and Joseph J Lim. Learning
 613 an embedding space for transferable robot skills. In *International Conference on Learning
 614 Representations (ICLR)*, 2018.

615 Irina Higgins, Loic Matthey, Arka Pal, Christopher Burgess, Xavier Glorot, Matthew Botvinick,
 616 Shakir Mohamed, and Alexander Lerchner. beta-vae: Learning basic visual concepts with a
 617 constrained variational framework. In *ICLR*, 2017.

618 Geoffrey E. Hinton and Ruslan R. Salakhutdinov. Reducing the dimensionality of data with neural
 619 networks. *Science*, 313(5786):504–507, 2006.

620 Yixin Hu, Jie Zhao, et al. Disentangled unsupervised skill discovery. *arXiv preprint
 621 arXiv:2410.11251*, 2024.

622 Seppo E Iso-Ahola. A theory of the skill-performance relationship. *Frontiers in Psychology*, 15:
 623 1296014, 2024.

624 Natasha Jacques, Angeliki Lazaridou, Edward Hughes, Caglar Gulcehre, Pedro A. Ortega,
 625 DJ Strouse, Joel Z. Leibo, and Nando de Freitas. Social influence as intrinsic motivation for
 626 multi-agent deep reinforcement learning. In *Proceedings of the 36th International Conference on
 627 Machine Learning (ICML)*, pp. 3040–3049. PMLR, 2019.

628 Hong Jun Jeon, Dylan P Losey, and Dorsa Sadigh. Shared autonomy with learned latent actions.
 629 *arXiv preprint arXiv:2005.03210*, 2020.

630 Hyunjik Kim and Andriy Mnih. Disentangling by factorising. *arXiv preprint arXiv:1802.05983*,
 631 2018.

632 Diederik P Kingma and Max Welling. Auto-encoding variational bayes. *arXiv preprint
 633 arXiv:1312.6114*, 2013.

634 Diederik P Kingma, Danilo J Rezende, Shakir Mohamed, and Max Welling. Semi-supervised learning
 635 with deep generative models. *Advances in neural information processing systems*, 27, 2014.

636 Yehuda Koren, Robert Bell, and Chris Volinsky. Matrix factorization techniques for recommender
 637 systems. In *Computer*, volume 42, pp. 30–37. IEEE, 2009.

638 Yann LeCun. A path towards autonomous machine intelligence. Position Paper, Version 0.9.2, jun
 639 2022. URL <https://openreview.net/forum?id=BZ5a1r-kVsf>. Courant Institute
 640 of Mathematical Sciences, New York University; Meta Fundamental AI Research.

648 Timothée Lesort, Natalia Díaz-Rodríguez, Jean-François Goudou, and David Filliat. State represen-
 649 tation learning for control: An overview. *Neural Networks*, 108:379–392, 2018.

650

651 Xingguo Lin, Kiran K. Thekumparampil, Giulia Fanti, and Sewoong Oh. Learning semantically
 652 meaningful embeddings using linear constraints. In *International Conference on Learning Rep-
 653 resentations (ICLR)*, 2020.

654 Francesco Locatello, Stefan Bauer, Mario Lucic, Gunnar Raetsch, Sylvain Gelly, Bernhard
 655 Schölkopf, and Olivier Bachem. Challenging common assumptions in the unsupervised learn-
 656 ing of disentangled representations. In *ICML*, pp. 4114–4124, 2019.

657 Samuel Messick. Validity of psychological assessment: Validation of inferences from persons’
 658 responses and performances as scientific inquiry into score meaning. *American Psychologist*, 50
 659 (9):741–749, 1995.

660 Karl M Newell. Motor skill acquisition. *Annual Review of Psychology*, 42(1):213–237, 1991.

661

662 Janith C Petangoda, Harshana Gammulle, Simon Denman, Clinton Fookes, Sridha Sridharan, et al.
 663 Disentangled skill embeddings for reinforcement learning. *arXiv preprint arXiv:1906.09223*,
 664 2019.

665 Chris Piech, Jonathan Bassen, Jonathan Huang, Surya Ganguli, Mehran Sahami, Leonidas Guibas,
 666 and Jascha Sohl-Dickstein. Deep knowledge tracing. In *Advances in Neural Information Pro-
 667 cessing Systems*, volume 28, 2015.

668

669 Richard A Schmidt, Timothy D Lee, Carole Winstein, Gabriele Wulf, and Howard N Zelaznik.
 670 *Motor Learning and Performance: From Principles to Application*. Human Kinetics, 2018.

671

672 Mariah Schrum, Allison Morgan, Deepak Gopinath, Jean Costa, Emily Sumner, Guy Rosman, and
 673 Tiffany Chen. A data-driven framework for skill representation. In *Proceedings of the 2025
 674 ACM/IEEE International Conference on Human-Robot Interaction (HRI)*, 2025. URL https://leap-hri.github.io/docs/LEAP-HRI_2025_paper_2.pdf. LEAP-HRI Work-
 675 shop.

676

677 David Snyder, Daniel Garcia-Romero, Gregory Sell, Daniel Povey, and Sanjeev Khudanpur. X-
 678 vectors: Robust dnn embeddings for speaker recognition. In *2018 IEEE International Conference
 679 on Acoustics, Speech and Signal Processing (ICASSP)*, pp. 5329–5333. IEEE, 2018.

680

681 Kihyuk Sohn, Honglak Lee, and Xinchen Yan. Learning structured output representation using deep
 682 conditional generative models. *Advances in neural information processing systems*, 28, 2015.

683

684 Y. Sun et al. Representation learning of human audio trajectories for person-level behavior modeling.
 685 *arXiv preprint arXiv:2407.16081*, 2024.

686

687 Aaron van den Oord, Yazhe Li, and Oriol Vinyals. Representation learning with contrastive predic-
 688 tive coding. *arXiv preprint arXiv:1807.03748*, 2018.

689

690 Sandra Varona-Moya, David Ariza-Villanueva, and Fernando García-Gil. Motor learning and the
 691 role of feedback in the implementation of motor skills. *Frontiers in Psychology*, 12:663234, 2021.

692

693 Yuxin Wu, Alexander Kirillov, Francisco Massa, Wan-Yen Lo, and Ross Girshick. Con-
 694 trastive learning of global and local features for temporal activity recognition. *arXiv preprint
 695 arXiv:2101.07862*, 2021.

696

697 Gabriele Wulf. Attentional focus and motor learning: a review of 15 years. *International Review of
 698 Sport and Exercise Psychology*, 9(1):77–104, 2016.

699

700 Shuochao Zhang, Han Li, Hongyang Gan, Liang Xu, and Xiaolong Zhang. Self-supervised learn-
 701 ing for human activity recognition using 700,000 accelerometer records. *IEEE Transactions on
 702 Mobile Computing*, 20(9):2424–2437, 2019.

703

704 Xiangyu Zhang, Han Yang, et al. A survey on disentangled representation learning. *arXiv preprint
 705 arXiv:2107.07176*, 2021.

706

707 Brian D Ziebart, Andrew Maas, J Andrew Bagnell, and Anind K Dey. Maximum entropy inverse
 708 reinforcement learning. In *AAAI*, pp. 1433–1438, 2008.

702 **A APPENDIX**
703704 **A.1 USE OF AI ASSISTANCE**
705706 Portions of the text in this paper were refined with the assistance of ChatGPT. The tool was used
707 only to improve clarity and readability of the manuscript and to aid in finding related works; all
708 ideas, experiments, and analyses are the authors' own.
709710 **A.2 ARCHITECTURE AND TRAINING DETAILS**
711712 **Skill embeddings.** Each participant is associated with a persistent, learnable skill vector $z_s \in \mathbb{R}^d$,
713 stored in an embedding table initialized from $\mathcal{N}(0, 0.1)$. For the racing domain, $d = 12$, partitioned
714 into six subskill slices: vehicle handling (3), gaze (3), inputs (3), know-how (1), physical (1), and
715 perception (1). For the baseball domain, $d = 7$, partitioned into kinematic chain (3), pause pelvis
716 (2), and pause thigh (2).
717718 **Map encoder.** For racing, we use a PointNet-Transformer encoder that processes local lane geom-
719 etry and produces per-segment encodings of dimension 64. This corresponds to the map encoder in
720 our formulation (Section 3). For baseball, no map input is used.
721722 **Blending decoders** g_ϕ . Behavior is represented as a blend of canonical expert and novice bases.
723 The *alpha decoder* maps (z_s, c) into elementwise interpolation weights α and predicts coefficients
724 for novice PCA bases grouped by feature (e.g., position, steering, throttle, brake, speed).
725726 **Skill predictor** q_ϕ . To regularize the latent space, we predict z_s from blending coefficients α using
727 a 2-layer Transformer encoder (hidden size 128, 4 heads, dropout 0.1) with a [CLS] token.
728729 **Trajectory-to-subskill predictor** h_{spi} . In addition to decoding metrics directly from z_s , we in-
730 clude a trajectory-to-subskill head h_{spi} that maps reconstructed trajectories \hat{r} into predicted subskill
731 metrics. This auxiliary supervision ties subskill metrics to observable behavior, complementing the
732 $z_s \mapsto m$ decoders. In practice, h_{spi} is implemented as a two-layer MLP applied to flattened trajectory
733 segments.
734735 **Training.** We train using Adam with learning rate 2×10^{-4} , weight decay 10^{-5} , batch size 256
736 (racing) or 5 (baseball), and a maximum of 2000 and 7000 epochs respectively. Losses include:
737 (i) trajectory reconstruction ($\lambda = 0.05$ –0.1), (ii) subskill metric decoding with h_ψ ($\lambda = 4.0$), (iii)
738 trajectory-to-subskill decoding with h_{spi} ($\lambda = 4.0$), (iv) trial time prediction ($\lambda = 0.1$ –2.0), and (v)
739 counterfactual supervision applied on 20% of batches. Auxiliary penalties include contrastive reg-
740 ularization ($\lambda = 1$), VICReg ($\lambda = 0.005$), orthogonality ($\lambda = 0.001$), and adversarial consistency
741 ($\lambda = 0.01$). Training was performed on NVIDIA RTX A6000 GPUs.
742743 **A.3 RACING DOMAIN AND SUBSKILL METRICS**
744745 Following prior work in HPDE (Schrum et al., 2025), we model racing expertise as a composition
746 of six subskills: *know-how*, *physical ability*, *gaze policy*, *vehicle handling*, *control inputs*, and *per-
747 ception*. Each subskill corresponds to a dedicated slice $z_s^{(k)}$ of the overall skill vector z_s , and is
748 supervised using behaviorally grounded metrics. Consistency is treated as a cross-cutting property
749 across subskills rather than a separate dimension.
750751 **Know-how.** Procedural and declarative knowledge of racing lines and techniques, assessed via a
752 written test (m_{know}).
753754 **Physical.** Motor ability and endurance, measured through grip strength and related assessments
755 (m_{phys}).
756757 **Gaze.** Visual attention strategies, measured via dispersion, dwell time, and fixation on apex cones
758 (m_{gaze}).
759760 **Vehicle handling.** Car control at the limit, measured through raceline deviation, lateral g-force, and
761 skidpad/slalom performance (m_{vh}).
762763 **Control inputs.** Coordination of steering, throttle, and braking, measured via steering reversal rate,
764 throttle smoothness, and braking stability (m_{inputs}).
765

756 **Perception.** Prediction and interpretation of the environment, assessed via occlusion tasks with
 757 hidden track segments (m_{perc}).
 758

759 Participants completed repeated lap blocks in a high-fidelity simulator, interleaved with drills (skid-
 760 pad, slalom, occlusion) and questionnaires. This design enables both between-subject discrimina-
 761 tion (novices vs. experts) and within-subject stability, allowing z_s to capture persistent skill while
 762 abstracting away transient performance fluctuations.

763 **A.4 EVALUATION METRICS**
 764

765 We provide details for the evaluation metrics reported in Section 5.1.
 766

767 **Silhouette score (↑):** Measures clustering quality of embeddings with respect to skill group. In
 768 the racing dataset, a subset of participants was labeled as experts or novices based on prior driving
 769 experience. Silhouette values compare within-group cohesion to between-group separation; higher
 770 values indicate that embeddings of the same skill group are tightly grouped and well-separated from
 771 others. Because analogous labels are not available for baseball, we omit this metric there.

772 A larger ratio reflects clearer separation between expert and novice embeddings in the latent space,
 773 providing an additional measure of construct validity.

774 **Test-retest similarity (↑):** Assesses temporal stability of embeddings across repeated trials from the
 775 same participant. We compute cosine similarity between embeddings estimated from independent
 776 subsets of trajectories. High values indicate that the representation reflects persistent aspects of skill
 777 rather than trial-specific noise.

778 **In-context behavior prediction (RMSE ↓):** Assesses how well z_s can be used to predict trajec-
 779 tories in the same context from which it was derived (e.g., skill inferred from laps on one racetrack
 780 and evaluated on the same track). Lower error indicates that the embedding captures fine-grained
 781 behavioral tendencies that persist within a given setting.

782 **Out-of-context (OOC) generalization error (RMSE ↓):** Evaluates predictive performance when
 783 applying z_s to novel contexts (e.g., skill inferred from behavior on one racetrack and tested on a
 784 different track). Lower error reflects better transfer, showing that the embedding encodes stable skill
 785 structure that generalizes beyond training conditions.

786 **Alignment Ratio (AR ↑):** Computed by training shallow linear probes on each subskill slice $z_s^{(k)}$
 787 to predict its corresponding behavioral metrics. AR measures how strongly the intended metric is
 788 predicted relative to non-target metrics. High AR values indicate that each slice encodes the correct
 789 factors with minimal cross-contamination.

790 **Targeted Change Index (TCI ↑):** Computed by performing counterfactual swaps of individual
 791 subskill slices and measuring changes in trajectory features. TCI quantifies the proportion of change
 792 concentrated in targeted features versus off-target leakage, with higher values indicating that slices
 793 selectively govern their intended behavioral dimensions.

794 **Relative Influence Ratio (RIR ↑):** Assesses the relative dominance of subskills on overlapping
 795 behavioral feature sets. For example, manipulating the control inputs subskill should strongly in-
 796 fluence brake/throttle/steering traces, while gaze manipulations should more strongly affect vehicle
 797 position. High RIR values indicate that the representation disentangles subskills while also capturing
 798 their relative strengths in shaping shared outputs.

799 **Composite Scores.** For each desideratum, we min–max normalize each constituent metric across
 800 methods (direction-corrected so higher is better) and sum the normalized values. The composite
 801 therefore ranges from 0 to the number of metrics in that desideratum (e.g., 2 for Predictive; 3 for
 802 Disentangle). In baseball, we omit Silhouette (no group labels), so Construct uses only test-retest
 803 (range 0–1). See Table 1 for the underlying metric values.

804 **A.5 BASEBALL DOMAIN RESULTS**
 805

806 While high-performance racing is our primary evaluation domain, we also tested **SAIL** on a supple-
 807 mental dataset of baseball hitting. This domain probes a different set of motor subskills and provides
 808 a test of cross-domain generalization. Because the dataset is smaller in scale and narrower in subskill

coverage, performance differences are less pronounced than in racing. Nevertheless, **SAIL** achieves the highest overall composite score, balancing predictive accuracy with disentanglement, whereas ablations highlight the trade-off between predictive utility (w/o CF) and interpretability.

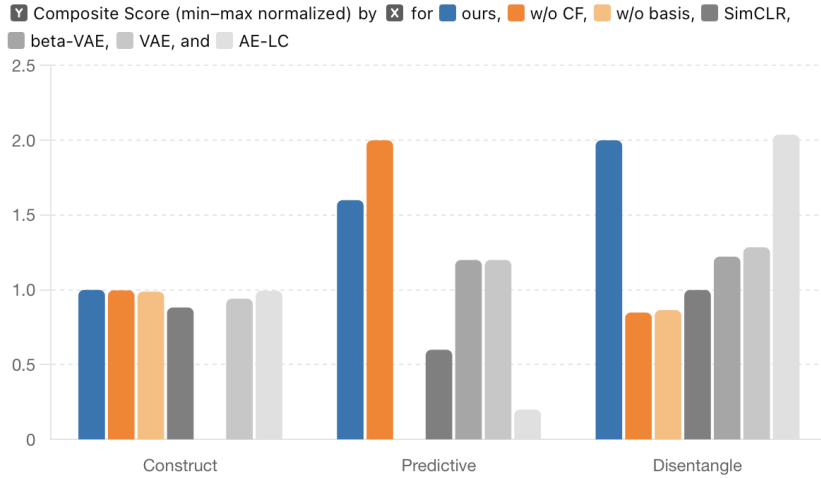


Figure 3: Composite scores across desiderata for the baseball domain. Bars show performance of our method (**SAIL**), ablations (w/o CF, w/o basis), and baselines (SimCLR, β -VAE, VAE, AE-LC). Although differences are smaller than in racing, **SAIL** maintains the best overall balance across desiderata.